Talanta 196 (2019) 420–428

Contents lists available at ScienceDirect

Talanta

journal homepage: www.elsevier.com/locate/talanta

In situ generation of hydrophobic magnetic ionic liquids in stir bar dispersive liquid-liquid microextraction coupled with headspace gas chromatography

María J. Trujillo-Rodríguez, Jared L. Anderson*

Department of Chemistry, Iowa State University, Ames, IA 50011, USA

ARTICLE INFO

Keywords:
Magnetic ionic liquids
In situ stir bar dispersive liquid-liquid microextraction
Gas chromatography
Mass spectrometry
Organic pollutants

ABSTRACT

For the first time, an *in situ* stir bar dispersive liquid-liquid microextraction approach has been developed and coupled with headspace gas chromatography-mass spectrometry for the determination of a group of organic pollutants. The method exploits a new generation of magnetic ionic liquids (MILs) that contain paramagnetic cations based on Ni^{2+} or Co^{2+} metal centers coordinated with either N-butylimidazole or N-octylimidazole ligands and chloride anions. The reactants are added to an aqueous solution containing a high field neodymium rod magnet, followed by the addition of the bis[(trifluoromethyl)sulfonyl]imide anion that promotes a metathesis reaction for the *in situ* generation of a hydrophobic MIL. Concurrently, a high stirring rate is maintained to exceed the magnetic field of the rod magnet and disperse the generated MIL in the sample solution. When stirring is stopped, the MIL coats the rod magnet due to its paramagnetic nature, facilitating the MIL transfer and subsequent desorption and analysis. Under optimum conditions, the method required a 2.5–18% (w/v) aqueous solution of sodium chloride, 10 mL of sample, 20 or 30 mg of MIL, the addition of a small volume of dispersive solvent, and stirring for 5–7.5 min, depending on the MIL. The method provided limits of detection (LODs) down to 10 μg L^{-1}, adequate reproducibility (with relative standard deviation values lower than 10% for a spiked level of 80 μg L^{-1}), and relative recoveries between 72.5% and 102%. Furthermore, the method was successfully applied in the analysis of tap and mineral water.

1. Introduction

The introduction of magnetic-assisted procedures in the field of sample preparation has significantly impacted analytical chemistry [1]. These methods generally exploit extraction materials with paramagnetic properties, allowing for their manipulation using external magnetic fields. Among the different microextraction techniques that have utilized magnetic separation, stir bar sorptive dispersive microextraction (SBSDME) [2,3] and stir bar dispersive liquid microextraction (SBDLME) [4,5] are of particular interest. Both techniques combine the advantages of stir bar sorptive extraction (SBSE) [6] with either solid-phase microextraction (SPME) [7] or dispersive liquid-liquid microextraction (DLLME) [8,9], respectively. These microextraction procedures involve the addition of extraction material to an aqueous solution containing a high field neodymium-rod magnet. A high stirring rate is set during the extraction to exceed the magnetic field of the rod magnet and disperse the extraction material within the sample solution. Stirring is then stopped, resulting in the magnetic material coating the rod magnet due its paramagnetic properties, facilitating its transfer to downstream analytical instrumentation. The main difference between these two techniques is the nature of the extraction material; that is, a solid sorbent is typically used in the case of SBSDME and a liquid solvent is used for SBDLME. For example, cobalt-ferrite magnetic nanoparticles have been used in SBSDME [2,3] whereas SBDLME has been demonstrated using magnetic ionic liquids (MILs) as extraction solvents [4,5].

MILs are a unique subclass of ionic liquids (ILs) that are specifically designed to contain a paramagnetic component in either the cation or anion [10,11]. MILs retain some properties of ILs, including low vapor pressure at room temperature and impressive solvation capabilities for a wide variety of analytes, from polar to non-polar compounds. These features makes MILs excellent solvents in sample preparation [12].

The MILs previously applied in SBDLME were based on phosphonium cation and anions consisting of metal centers coordinated with the hexafluoroaceylacetonate ligand [4,5]. This generation of MILs possess low viscosity (299–928 cP at 23.7 °C [13]), high chemical stability and high magnetic susceptibility (2.8–9.7 μ_B), and are advantageous over tetrachloroferrate(III) ($[FeCl_4^-]$) and bromotrichloroferrate(III) ($[FeBrCl_3^-]$)-based MILs, which exhibit hydrolysis when exposed to aqueous solutions [4,5,14–17]. Recently, a new generation of MILs

---

* Correspondence to: Department of Chemistry, Iowa State University, 1605 Gilman Hall, Ames, IA 50011, USA.
E-mail address: andersoj@iastate.edu (J.L. Anderson).

https://doi.org/10.1016/j.talanta.2018.12.071
Received 22 November 2018; Received in revised form 21 December 2018; Accepted 21 December 2018

Table 1
Optimum extraction conditions obtained for the *in situ* SBDLLME-HS-GC-MS method with different MILs.

Parameter[a]	**MIL**		
	$[Ni(C_4IM)_4^{2+}]\,2\,[Cl^-]$	**$[Ni(C_8IM)_4^{2+}]\,2\,[Cl^-]$**	**$[Co(C_8IM)_4^{2+}]\,2\,[Cl^-]$**
NaCl content	18% (w/v)	4.6% (w/v)	2.5% (w/v)
pH	2	2	2
Amount of MIL	20 mg	30 mg	20 mg
Type of dispersive solvent	Tetrahydrofuran: Acetone (50:50%, v/v)	Tetrahydrofuran	Tetrahydrofuran
Volume of dispersive solvent	600 µL	400 µL	600 µL
Extraction time	5 min	7.5 min	5 min
HS temperature[b]	150 °C	175 °C	140 °C
HS time	20 min	10 min	10 min
HS vial volume	6 mL	6 mL	6 mL

[a] The following parameters were fixed during the optimization of all MILs: sample volume, 10 mL; MIL:$[Li^+][NTf_2^-]$ molar ratio, and the stirring rate, 1150 rpm.
[b] The loop and the transfer line in the HS system were maintained 15 °C and 25 °C higher than the sampling temperature, respectively.

containing paramagnetic cations has been introduced [18]. In particular, these MILs are based on cations containing a paramagnetic metal center (*i.e.* Ni^{2+}, Co^{2+} or Mn^{2+}) coordinated with four N-alkylimidazole ligands. The MILs possess low viscosity (680–2501 cP at 21.7 °C [18]) and have a lower tendency to stick on glass. Another important advantage of these MILs is the possibility to easily tune the MIL chemical structure by either changing the metal center or the N-alkylimidazole ligand. These small modifications can result in dramatic changes for some important features of the MIL, including chemical stability, solubility, viscosity, and thermal stability. In addition, hydrophobic MILs based on these paramagnetic cations can be generated *in situ* during the microextraction procedure, resulting in their use for *in situ* DLLME studies [19].

In this study, we report for the first time an *in situ* stir bar dispersive liquid-liquid microextraction (SBDLLME) method using three different MILs containing Ni^{2+} or Co^{2+} metal centers coordinated with N-butylimidazole or N-octylimidazole ligands as extraction solvents. The dispersion of the MIL was achieved by (*1*) using a small volume of organic solvent, (*2*) applying high stirring rates during the extraction, and (*3*) performing metathesis reaction between the MIL initially in the chloride-form to generate the bis[(trifluoromethyl)sulfonyl]imide ($[NTf_2^-]$)-based compound, *in situ* generating a hydrophobic MIL that can be subsequently collected by the rod magnet used as stir bar. The microextraction method was combined with headspace gas chromatography mass spectrometry (HS-GC-MS) for the determination of a group of organic pollutants in water samples.

2. Materials and methods

2.1. Chemicals, reagents, materials and samples

A group of 7 organic pollutants was determined in this study. Naphthalene (Nap, 99%), acenaphthene (Ace, analytical standard), and fluorene (Fl, analytical standard) were purchased from Supelco (Bellefonte, PA, USA). The analytes 1-chloro-4-nitrobenzene (CNB, 99%), biphenyl (Bip, 99.5%), and 5-bromoacenaphthene (BAce, analytical standard) were obtained from Sigma-Aldrich (St. Louis, MO, USA), and 3-tert-butylphenol (tBP, 99%) was purchased from Alfa Aesar (Tewksbury, MA, USA).

Individual stock solutions were prepared in acetonitrile at 5000 mg L^{-1}. An intermediate stock solution containing all analytes was prepared in acetonitrile at a concentration of 150 mg L^{-1} by dilution of the individual stock solutions. Standard working solutions were prepared by dilution of the intermediate stock solution in ultrapure water resulting in final concentrations between 2.0 and 1000 µg L^{-1}. Ultrapure water (18.2 MΩ cm) was obtained from a Milli-Q water purification system (Millipore, Bedford, MA, USA).

The reagents N-butylimidazole (98%), $NiCl_2$ (98%) and $CoCl_2{\cdot}6H_2O$ (98%) were purchased from Sigma-Aldrich. N-octylimidazole (98%) was purchased from IoLiTec Inc (Tuscaloosa, AL, USA).

The following three MILs were used as extraction solvents: tetrabutylimidazolenickelate(II) chloride ($[Ni(C_4IM)_4^{2+}]2[Cl^-]$), tetraoctylimidazolenickelate(II) chloride ($[Ni(C_8IM)_4^{2+}]2[Cl^-]$), and tetraoctylimidazolecobaltate(II) chloride ($[Co(C_8IM)_4^{2+}]2[Cl^-]$). The MILs were dissolved in water or an appropriate organic solvent, depending on the experiment.

Acetonitrile, methanol, acetone, and tetrahydrofuran (HPLC grade) were obtained from Sigma-Aldrich. Sodium chloride, sodium hydroxide, hydrochloric acid and tetrahydrofuran (certified ACS reagents) were purchased from Fisher Scientific (Fair Lawn, NJ, USA). Lithium bis[(trifluoromethyl)sulfonyl]imide ($[Li^+][NTf_2^-]$) was purchased from SynQuest Laboratories (Alachua, FL, USA). An aqueous solution of $[Li^+][NTf_2^-]$ (400 mg L^{-1}) was used during the *in situ* SBDLLME procedure.

2.2. Instrumentation

A 7890B GC from Agilent Technologies (Santa Clara, CA, USA) hyphenated with a 5977A MS detector (single quadrupole) and a 7697A HS sampler unit was used for all analyses. The HS sampler was operated in fill mode (flow to pressure, 50 psi). No stirring was performed during HS sampling. The remaining HS sampler conditions are detailed in Table 1. The GC separation was carried out in a HP-5ms ultra inert capillary column from Agilent Technologies (30 m L × 0.250 mm I.D. × 0.25 µm of film thickness). Ultrapure helium was used as carrier gas at a flow rate of 1 mL min^{-1}. The inlet was maintained at 290 °C with a 5:1 split ratio. The following temperature program was employed: initial temperature of 90 °C; the temperature was increased at 4 °C min^{-1} up to 206 °C; followed by an increase at 20 °C min^{-1} to 290 °C, and held for 2 min. The transfer line from the GC to the MS was maintained at 250 °C. The MS was operated in electron ionization (EI) mode at 70 eV using 230 °C and 150 °C as the source and quadrupole temperatures, respectively. Data was acquired using single ion monitoring (SIM). All analytes were identified by considering their retention time, the presence of two characteristic ions of each analyte (termed as quantifier and qualifier ions), and their ratio. For quantitative purposes, the peak area of the quantifier ion was used. Table S1 of the Supplementary Material (SM) shows the segment program utilized in the MS, the retention time, and the two ions considered for each analyte.

2.3. Procedures

2.3.1. Synthesis of magnetic ionic liquids

The MILs were synthesized according to a previously reported method, with some modifications [18]. The $[Ni(C_4IM)_4^{2+}]2[Cl^-]$ MIL was prepared by reacting 4.0 mmol of $NiCl_2$ with 16 mmol of N-butylimidazole overnight at room temperature in water.

The $[Ni(C_8IM)_4^{2+}]2[Cl^-]$ and $[Co(C_8IM)_4^{2+}]2[Cl^-]$ MILs were prepared by reacting 4.0 mmol of $NiCl_2$ (or $CoCl_2$) with 16 mmol of N-octylimidazole overnight at 100 °C. The reaction mixture was then dissolved in 10 mL of methanol and refluxed for 24 h at 60 °C. For preparation of MILs containing N-octylimidazole ligands, both the hydrated $NiCl_2$ and $CoCl_2$ salts were dried in a vacuum oven for 4 days at 50 °C. The composition of the obtained MILs was found to be consistent with the $[M(C_nIM)_4^{2+}]2[Cl^-]$ form (with M = Ni or Co, and n = 4 or 8) based on elemental analysis [18].

2.3.2. In situ stir-bar dispersive liquid-liquid microextraction procedure

A sample volume of 8.2–9.8 mL (or aqueous standard solution) containing 0–22% (w/v) NaCl was placed in a 20 mL vial and the pH was adjusted to 2–8 with 0.5 M HCl or 0.5 M NaOH. A NdFeB rod magnet (3.2–6.4 mm diameter × 12.7 mm length, axially or diametrically magnetized) from K&J Magnetics, Inc. (Pipersville, PA, USA) was introduced in the extraction vial. The stirring rate was set to 600 rpm and 20–60 mg of MIL and 200–800 mL of dispersive solvent (acetone, acetonitrile or tetrahydrofuran) was subsequently added to the vial. A volume between 21.5 and 129 µL of the ion-exchange reagent ($[Li^+][NTf_2^-]$, 400 mg L^{-1}) was then added to achieve a 1:2 MIL:$[Li^+][NTf_2^-]$ molar ratio, and the stirring rate was increased to 1150 rpm for 5–25 min. The total volume was 10 mL in all experiments. During stirring, the MIL (in the $[NTf_2^-]$-form generated from the metathesis reaction) was dispersed within the extraction vial. When the stirring was stopped, the hydrophobic MIL immediately settled to the bottom of the vial and was collected onto the NdFeB rod magnet. Finally, the MIL-coated rod magnet was transferred using plastic tweezers to a 10 mL HS vial or a modified HS vial of 6 mL, and subjected to HS sampling at 100–200 °C for 10–40 min. The optimum conditions used for each MIL are detailed in Table 1. A video of the procedure has also been included within the SM.

Modified HS vials containing a 6 mL HS volume were designed according to previously reported methods [15,20]. 10 mL HS glass vials (Agilent Technologies) were filled with 10.8 g of glass beads (3 mm diameter), and a flat bottom glass insert was placed inside the vial. The vial was sealed with a crimped silver aluminum cap containing a polytetrafluoroethylene (PTFE)/silicone septum (Agilent Technologies).

3. Results and discussion

3.1. Selection of magnetic ionic liquids and optimization of headspace sampling

Three different MILs were used as extraction solvents in this approach, including $[Ni(C_4IM)_4^{2+}]2[Cl^-]$, $[Ni(C_8IM)_4^{2+}]2[Cl^-]$ and $[Co(C_8IM)_4^{2+}]2[Cl^-]$. These MILs were selected in order to study the effect of both different metal centers (Ni^{2+} or Co^{2+}) and N-alkylimidazole ligands (C_4IM or C_8IM) on the extraction efficiency of the method.

In a recently reported method, the $[Ni(C_4IM)_4^{2+}]2[NTf_2^-]$ MIL was applied in *in situ* DLLME and directly combined with reversed-phase high performance liquid chromatography (RP-HPLC) using a mobile phase composed of acetonitrile and formic acid (pH 3) [19]. In this approach, the MIL eluted at the beginning of the elution program. However, the presence of longer alkyl chains substituents within the N-alkylimidazole ligand (*e.g.* C_8) and the use of Co^{2+} centers instead of Ni^{2+} caused an increase in the hydrophobicity of the MIL in both the $[Cl^-]$- or $[NTf_2^-]$-forms, preventing their direct injection in HPLC. Considering the volatile or semi-volatile nature of the studied analytes, this approach involved an extra thermal desorption step from the analyte-enriched MIL-coated rod magnet. This step was carried out using a HS sampler directly connected to a GC-MS, which can be beneficial in cases where complete automation of the procedure is desired. The main aim of this step was to achieve adequate back-extraction of the analytes without any volatilization or decomposition of the MIL, thereby ensuring complete GC-MS compatibility. Therefore, 20 mg of each MIL in the $[NTf_2^-]$-form was directly added to a 10 mL HS vial and subjected to HS-GC-MS using HS sampling temperatures ranging between 100 and 225 °C. The GC-MS was operated in scan mode and ions were registered in the 40–900 *m/z* range. A detail explanation of the extraction conditions is shown in Table S2 of the SM. At lower HS sampling temperatures, no peaks originating from MIL degradation were observed in the chromatograms. When the $[Ni(C_4IM)_4^{2+}]2[NTf_2^-]$ MIL was analyzed, a degradation peak was observed when 175 °C or higher HS sampling temperatures was used. The peak was identified as N-butylimidazole using the 2014 NIST/EPA/NIH mass spectral library. Thus, a maximum operating HS temperature of 150 °C was selected for this MIL. Fig. S1 of the SM shows representative examples of the obtained chromatograms for this MIL at different HS sampling temperatures. Similarly, 200 °C and 140 °C were selected for the $[Ni(C_8IM)_4^{2+}]2[NTf_2^-]$ and $[Co(C_8IM)_4^{2+}]2[NTf_2^-]$ MILs, respectively.

Once the maximum operating HS sampling temperatures were defined, the most important parameters influencing HS sampling were optimized, including the HS temperature, time and volume. No stirring was performed during HS sampling to prevent rupture of the vials in the sampler due to the impact of the rod magnet with the vial walls. The extraction conditions utilized for the optimization of the HS parameters were the following: for all MILs, 10 mL of sample, 1:2 MIL:$[Li^+][NTf_2^-]$ molar ratio, and stirring (1150 rpm, 5 min) was used. A concentration of 20% (w/v) of NaCl, 40 mg of MIL and 600 µL of acetone was employed when the $[Ni(C_4IM)_4^{2+}]2[Cl^-]$ MIL was used; 4.6% (w/v) of NaCl, 30 mg of MIL and 800 µL of acetonitrile when the $[Ni(C_8IM)_4^{2+}]2[Cl^-]$ MIL was used; and 2.5% (w/v) of NaCl, 30 mg of MIL and 600 µL of tetrahydrofuran when the $[Ni(C_8IM)_4^{2+}]2[Cl^-]$ MIL was employed.

3.1.1. Headspace sampling temperature

The effect of HS sampling temperature was studied from 100 °C to the maximum operating temperature of each MIL (see Table S2 of the SM). Fig. S2 of the SM shows the obtained results. Temperatures of 150 °C, 175 °C, and 140 °C were selected for the $[Ni(C_4IM)_4^{2+}]2[Cl^-]$, $[Ni(C_8IM)_4^{2+}]2[Cl^-]$, and $[Co(C_8IM)_4^{2+}]2[Cl^-]$ MILs, respectively. In the case of the $[Ni(C_4IM)_4^{2+}]2[Cl^-]$ and $[Co(C_8IM)_4^{2+}]2[Cl^-]$ MILs, lower HS temperatures than the selected values provided little to no desorption of the analytes. However, the $[Ni(C_8IM)_4^{2+}]2[Cl^-]$ MIL exhibited different behavior; in this case, the extraction efficiency was observed to increase from 150 to 175 °C and then decreased at higher temperatures. This decrease was likely due to a shift of the partition coefficients of the analytes from the MIL to the HS at elevated temperatures, and is in agreement with previously reported methods [20,21].

3.1.2. Headspace sampling time

The HS time plays an important role in the HS sampling step. Shorter times may not be sufficient for adequate desorption of analytes from the MIL-coated rod magnet, whereas longer sampling times may cause re-absorption of the analytes in the MIL. In this approach, the HS time was studied in the range between 10 and 40 min. The results are presented in Fig. S3 of the SM. When the $[Ni(C_4IM)_4^{2+}]2[Cl^-]$ MIL was used, the maximum extraction efficiency was achieved in 20 min. HS times lower or higher than this value caused a decrease in the extraction efficiency, likely due to the aforementioned reasons. Different behavior was observed using the $[Ni(C_8IM)_4^{2+}]2[Cl^-]$ MIL. In this case, increasing the HS time decreased the extraction efficiency for all analytes. The same behavior was observed for CNB and tBP when the $[Co(C_8IM)_4^{2+}]2[Cl^-]$ MIL was used. For the remaining analytes, there was no significant change in the extraction efficiency. Based on these results, the selected optimum HS times were 20 min for the $[Ni(C_4IM)_4^{2+}]2[Cl^-]$ MIL and 10 min for the $[Ni(C_8IM)_4^{2+}]2[Cl^-]$ and $[Co(C_8IM)_4^{2+}]2[Cl^-]$ MILs.

3.1.3. Influence of headspace volume

The HS volume is directly related to the preconcentration of the

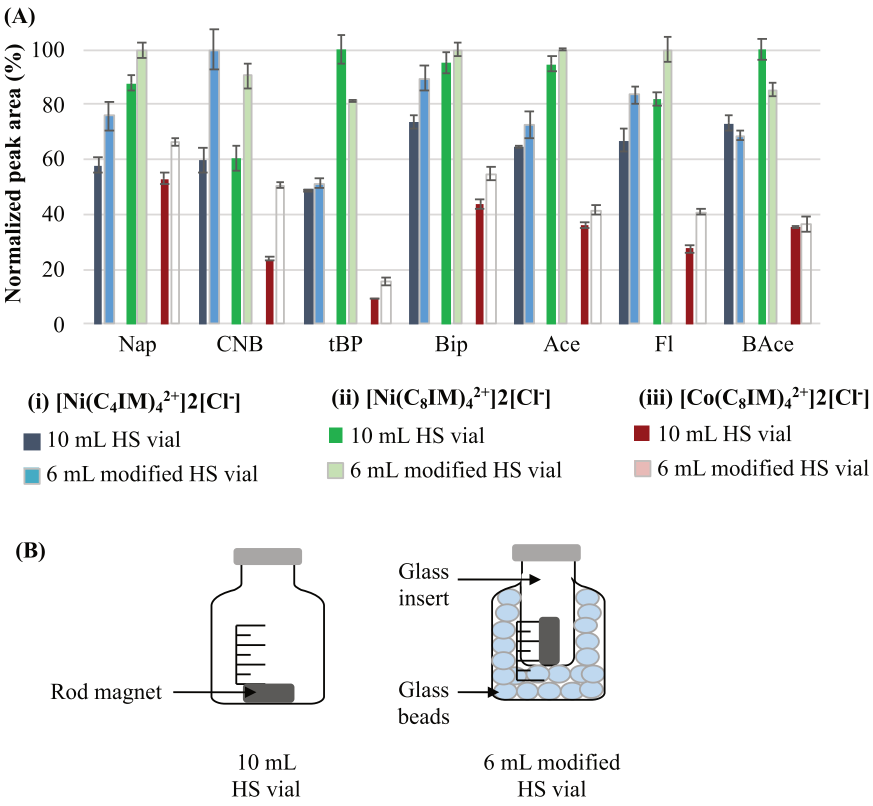

Fig. 1. (A) Effect of the HS sampling volume on the *in situ* SBDLLME method using the (i) $[Ni(C_4IM)_4^{2+}]2[Cl^-]$, (ii) $[Ni(C_8IM)_4^{2+}]2[Cl^-]$, and (iii) $[Co(C_8IM)_4^{2+}]2[Cl^-]$ MILs. *Experimental conditions* (n = 3): *For all experiments:* 10 mL sample volume, 500 µg L^{-1} as spiked level, pH 2, 1:2 MIL: $[Li^+][NTf_2^-]$ molar ratio, and 6–10 mL HS vials. *Specific extraction conditions:* (i) 18% (w/v) NaCl, 20 mg of MIL, 600 µL of tetrahydrofuran: acetone (50:50, v/v), stirring (1150 rpm, 5 min); and HS sampling (150 °C, 20 min); (ii) 4.6% (w/v) of NaCl, 30 mg of MIL, 400 µL of tetrahydrofuran, stirring (1150 rpm, 7.5 min), and HS sampling (175 °C, 10 min); and (iii) 2.5% (w/v) of NaCl, 20 mg of MIL, 600 µL of tetrahydrofuran, stirring (1150 rpm, 5 min), and HS sampling (140 °C, 10 min). (B) Scheme of commercial HS vials of 10 mL and the developed 6 mL modified vials.

method and, therefore, it affects the extraction efficiency. Lower HS volumes provide higher extraction efficiency, as demonstrated in previously reported methods [15,20,22]. The effect of this parameter was studied by performing experiments at HS volumes of 6 and 10 mL. For experiments using 10 mL, the MIL-coated rod magnet was directly introduced into the smallest commercially available HS vials with a 10 mL capacity. To reduce the HS volume to 6 mL, the 10 mL vials were filled with glass beads and a glass insert was added, as shown in Fig. 1(B). The developed vials had space for placing the MIL-coated rod magnet, and they were big enough to prevent contamination of the HS sample probe. When these modified HS vials were used, an increase in the extraction efficiency was observed for all analytes and MILs (see Fig. 1(A)), with the exception of tBP and BAce with the Ni-based MILs. In these cases, either no change or a slight decrease in the extraction efficiency was observed. An optimum HS volume of 6 mL was selected for all MILs.

3.2. Optimization of in situ stir bar dispersive liquid-liquid microextraction procedure

The *in situ* SBDLLME procedure was optimized for the three studied MILs. The studied parameters included the type of rod magnet, amount of MIL, ionic strength and pH, type and volume of dispersive solvent, and stirring time. Table 1 shows the selected optimum parameters obtained for each MIL. A sample volume of 10 mL was fixed in all cases to achieve adequate preconcentration. A 1:2 MIL to $[NTf_2^-]$ molar ratio was selected as optimum according to the results obtained in a previously reported method using similar MILs for *in situ* DLLME [19]. The final stirring step was fixed to the maximum speed of the magnetic stirrer (1150 rpm) to exceed the magnetic field of the rod magnet and disperse the *in situ* generated hydrophobic MIL within the sample solution.

3.2.1. Influence of rod magnet used as stir bar during the microextraction procedure

The characteristics of rod magnets used as stir bars are very important in the *in situ* SBDLLE procedure. In particular, the size and magnetization of the magnet affect the separation step, which can directly influence the extraction efficiency and reproducibility. For that reason, experiments were performed using three different sizes of NdFeB rod magnets (*small*, 3.2 mm of diameter (D); *medium*, 4.8 mm D; and *large*, 6.4 mm D). The influence of magnetization direction of the magnet was also considered by studying both axially and diametrically magnetized magnets. Axial magnets are those magnetized along their geometric axis whereas diametrical magnets are magnetized across their diameter. Fig. S4 of the SM shows a scheme of these two types of magnets, and the results obtained after performing these experiments with the $[Ni(C_4IM)_4^{2+}]2[Cl^-]$ MIL. In general, no significant differences in the extraction efficiency were observed using these studied magnets. Slightly lower extraction efficiency was achieved using *small* axially magnets for Nap, Fl, and BAce, and using *medium* diametrically or *large* axially magnetized magnets for CNB and tBP. However, important operational differences were observed depending on the magnet. These differences affected the reproducibility, extraction time, and the subsequent compatibility of the procedure with HS-GC-MS, especially with regard to the magnetization direction. It was observed that magnet collection using tweezers was easier and faster with axially magnetized magnets as the majority of the MIL coated the tips of the magnet (see Fig. S4(B)). Therefore, *medium* axially magnetized magnets were selected for subsequent experiments.

3.2.2. Mass of MIL

The effect of amount of MIL was studied in the range between 20 and 60 mg for each MIL, as shown in Fig. 2. In the case of the $[Ni(C_4IM)_4^{2+}]2[Cl^-]$ MIL, the highest extraction efficiencies were achieved in the majority of cases using 20 mg of MIL. The use of higher amounts of MIL generally reduced the extraction efficiency. In these cases, larger volumes of MIL were generated during the microextraction procedure, decreasing the preconcentration factor. The exceptions were Nap and tBP for which the highest normalized peak areas were obtained using 30 mg. An amount of 20 mg of $[Ni(C_4IM)_4^{2+}]2[Cl^-]$ was selected as

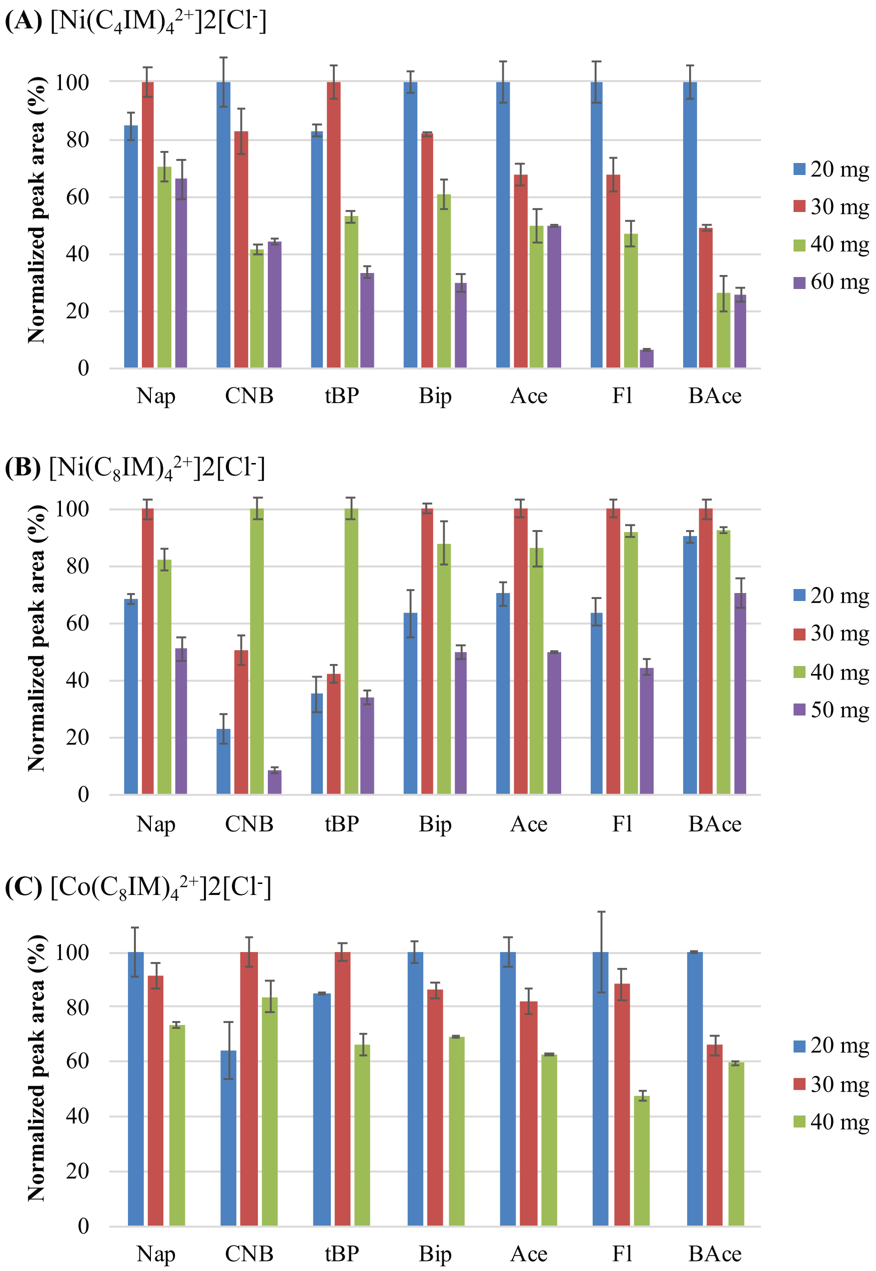

Fig. 2. Effect of the amount of MIL in the *in situ* SBDLLME method using (A) $[Ni(C_4IM)_4{}^{2+}]2[Cl^-]$, (B) $[Ni(C_8IM)_4{}^{2+}]2[Cl^-]$, and (C) $[Co(C_8IM)_4{}^{2+}]2[Cl^-]$. *Experimental conditions* (n = 3): *For all experiments:* 10 mL sample volume, 500 µg L^{-1} as spiked level, pH 2, 20–60 mg of MIL, 1:2 MIL:$[Li^+][NTf_2{}^-]$ molar ratio, and stirring (1150 rpm, 5 min). *Specific extraction conditions:* (A) 20% (w/v) NaCl and 600 µL of acetone; (B) 4.6% (w/v) of NaCl and 800 µL of acetonitrile; and (C) 2.5% (w/v) of NaCl, and 600 µL of tetrahydrofuran.

optimum.

Experiments regarding the use of the $[Ni(C_8IM)_4{}^{2+}]2[Cl^-]$ MIL (Fig. 2(B)) revealed that a higher amount of MIL was required: namely, 40 mg for CNB and tBP and 30 mg for the remaining analytes. Lower amounts of MIL provided lower extraction efficiency due to saturation of the MIL. Similar behavior was observed for the $[Co(C_8IM)_4{}^{2+}]2[Cl^-]$ MIL (Fig. 2(C)), for which 30 mg was required to achieve the highest extraction efficiency in the case of CNB and tBP, and 20 mg for the remaining analytes. In view of these results, 30 mg and 20 mg were selected as optimum values for the $[Ni(C_8IM)_4{}^{2+}]2[Cl^-]$ and $[Co(C_8IM)_4{}^{2+}]2[Cl^-]$ MILs, respectively.

3.2.3. NaCl content and pH of aqueous solution

Increasing the ionic strength has two different effects in the *in situ* SBDLLME procedure. On one hand, it can decrease the solubility of the MIL in both the $[Cl^-]$- and the $[NTf_2{}^-]$-form, directly affecting the microdroplet volume that coats the rod magnet after extraction. In addition, it can promote faster partitioning of the analytes to the *in situ* generated MIL due to the salting out effect [4]. For that reason, the effect of ionic strength was studied by the addition of NaCl at different concentrations ranging from 0% to 22% (w/v), depending on the MIL, and using the optimum amount of each MIL (see Section 3.2.2). The obtained results are shown in Fig. S5 of the SM. In the case of the $[Ni(C_4IM)_4{}^{2+}]2[Cl^-]$ MIL, 10% (w/v) NaCl was required to obtain reproducible results using the optimum amount of MIL (20 mg). The extraction efficiency was observed to increase from 10% to 18% (w/v) due to the salting out effect, and then decreased when higher concentrations were used, likely due to a decrease of the MIL solubility, which generated higher microdroplet volumes. For that reason, 18% (w/v) NaCl was selected as optimum. The effect of the NaCl content using the $[\mathrm{Ni(C_8IM)_4}^{2+}]2[\mathrm{Cl}^-]$ and $[\mathrm{Co(C_8IM)_4}^{2+}]2[\mathrm{Cl}^-]$ MILs was different due to the higher hydrophobicity of these MILs. A minimum value of 2.5% (w/v) NaCl was required to obtain reproducible results with the $[\mathrm{Ni(C_8IM)_4}^{2+}]2[\mathrm{Cl}^-]$ MIL, while experiments with the $[\mathrm{Co(C_8IM)_4}^{2+}]2[\mathrm{Cl}^-]$ MIL in ultrapure water were possible using the optimum MIL amounts. Values higher than 7.5% (w/v) were avoided as they resulted in partial insolubilization of the MIL in the $[\mathrm{Cl}^-]$-form, which significantly increased the required time for performing the metathesis reaction and reduced the extraction efficiency. For the $[\mathrm{Ni(C_8IM)_4}^{2+}]2[\mathrm{Cl}^-]$ MIL, the maximum extraction efficiency was obtained using 4.6% (w/v) NaCl (with the exception of NaP) whereas 2.5% (w/v) NaCl provided better results using the $[\mathrm{Co(C_8IM)_4}^{2+}]2[\mathrm{Cl}^-]$ MIL (with the exception of tBP).

The influence of sample pH was studied for the $[\mathrm{Ni(C_4IM)_4}^{2+}]2[\mathrm{Cl}^-]$ MIL in the range between 2 and 8. The sample pH was adjusted by adding HCl or NaOH, depending on the experiments. The results, presented in Fig. S6 of the SM, showed a slight increase in extraction efficiency at pH 2 for Bip, Ace, Fl, and BAce. These results are related to the stability of the metal complexes of the MIL cation [23,24]. Lower pH values increased the stability of the complexes, whereas basic pH values may have resulted in the formation of hydroxylated complexes with the Ni^{2+} cations, causing a decrease in the extraction efficiency [19]. In view of these results, pH 2 was selected as optimum for all MILs.

3.2.4. Dispersive solvent type and volume

The addition of a dispersive solvent was found to be beneficial for the dispersion and formation of hydrophobic MIL during the metathesis reaction [19]. Furthermore, in the case of MILs containing $\mathrm{C_8IM}$ as ligands, the dispersive solvent also increased the solubility of the initial extraction material in the $[\mathrm{Cl}^-]$-form. For these reasons, the effect that different solvents including acetonitrile, acetone, and tetrahydrofuran (THF) exert in the extraction efficiency was studied. In addition, different dispersive solvent mixtures containing THF and acetone, or THF and acetonitrile (depending on the MIL) were also considered. Fig. 3 shows the obtained results for the $[\mathrm{Ni(C_4IM)_4}^{2+}]2[\mathrm{Cl}^-]$ MIL. In this case, the maximum extraction efficiency was achieved using a mixture of THF: acetone (50:50, v/v) for Bip, Ace, Fl, and BAce; THF: acetone (75:25, v/v) for Nap and CNB; and acetone for tBP. A dispersive solvent mixture composed of THF: acetone (50:50, v/v) was selected as the optimum solvent for this MIL. Tetrahydrofuran was selected for the remaining MILs according to the obtained results, as shown in Fig. S7 of the SM.

The effect of dispersive solvent volume was also studied in the range between 200 and 800 μL, as shown in Fig. S8 of the SM. The behavior of all MILs was similar regarding the dispersive solvent volume as the extraction efficiency was observed to increase with the dispersive solvent volume until reaching a maximum, and then decreased at higher volumes. These results can be attributed to the fact that small dispersive solvent volumes did not properly disperse the MIL in the sample, whereas higher volumes could partially dissolve the hydrophobic MIL. The maximum extraction efficiency using the $[\mathrm{Ni(C_4IM)_4}^{2+}]2[\mathrm{Cl}^-]$ MIL was achieved by employing 400 μL for Nap, CNB and tBP, and 600 μL for the remaining analytes. Similarly, 400 and 600 μL were generally required when the $[\mathrm{Ni(C_8IM)_4}^{2+}]2[\mathrm{Cl}^-]$ and $[\mathrm{Co(C_8IM)_4}^{2+}]2[\mathrm{Cl}^-]$ MILs, respectively, were employed. The optimum selected values were 400 μL for the $[\mathrm{Ni(C_8IM)_4}^{2+}]2[\mathrm{Cl}^-]$ MIL, and 600 μL for the remaining MILs.

3.2.5. Influence of stirring time

The stirring step using the rod magnet at high speed (1150 rpm) is a parameter of major importance in this procedure as it can affect the metathesis reaction and the dispersion of the generated hydrophobic MIL. The influence of stirring time was studied in the range between 5 and 25 min, depending on the MIL. The obtained results are presented in Fig. S9 of the SM. Experiments for all MILs revealed that, in general, shorter stirring times provided higher extraction efficiency. In these cases, the stirring accelerated the metathesis reaction, promoting fast mass transfer of the analytes to the *in situ* generated MIL. Longer extraction times provide either no change or a slight decrease in the extraction efficiency, depending on the analyte and MIL, likely due to stability issues of the MIL at long extraction times [23,24]. Based on these results, 5 min was selected as optimum for the $[\mathrm{Ni(C_4IM)_4}^{2+}]2[\mathrm{Cl}^-]$ and $[\mathrm{Co(C_8IM)_4}^{2+}]2[\mathrm{Cl}^-]$ MILs and 7.5 min for the $[\mathrm{Ni(C_8IM)_4}^{2+}]2[\mathrm{Cl}^-]$ MIL.

3.3. Analytical performance

Once the method was optimized, it was validated by developing the corresponding calibration curves. Tables S3, S4 and S5 of the SM include several of the analytical figures of merits obtained after performing these experiments. Furthermore, Table 2 shows the linear ranges, limits of detection (LODs), reproducibility, and relative recovery (RR).

Wide linearity varying from 15 to 50 $\mu\mathrm{g\,L^{-1}}$ to 800–1000 $\mu\mathrm{g\,L^{-1}}$ was achieved, depending on the analyte and the MIL (see Table 2). The narrowest linear ranges were achieved using the $[\mathrm{Co(C_8IM)_4}^{2+}]2[\mathrm{Cl}^-]$ MIL.

The calibration slopes of the analytes are shown in Fig. 4. These values are directly related with the sensitivity of the method. The calibration slopes ranged between $(1.08 \pm 0.04)\cdot10^2$ and $(30.1 \pm 0.7)\cdot10^2$ for the $[\mathrm{Ni(C_4IM)_4}^{2+}]2[\mathrm{Cl}^-]$ MIL, from $(1.6 \pm 0.1)\cdot10^2$ and $(49 \pm 2)\cdot10^2$ for the $[\mathrm{Ni(C_8IM)_4}^{2+}]2[\mathrm{Cl}^-]$ MIL, and from $(0.21 \pm 0.01)\cdot10^2$ and $(32.3 \pm 0.9)\cdot10^2$ for the $[\mathrm{Co(C_8IM)_4}^{2+}]2[\mathrm{Cl}^-]$ MIL. The sensitivity was the lowest for BAce, tBP, and CNB, depending on the MIL, and maximum for Nap in the case of all MILs. Comparing the results with all MILs, the highest calibration slopes were obtained with the $[\mathrm{Ni(C_8IM)_4}^{2+}]2[\mathrm{Cl}^-]$ MIL (with the exception of CNB), with calibration slopes between 1.3 and 2.6 and 1.5–20 times higher than the $[\mathrm{Ni(C_4IM)_4}^{2+}]2[\mathrm{Cl}^-]$ and $[\mathrm{Co(C_8IM)_4}^{2+}]2[\mathrm{Cl}^-]$ MILs, respectively. If the MILs containing Ni^{2+} metal centers are compared, the obtained results indicated that the presence of long alkyl chains within the ligands of the MIL cation was beneficial for the

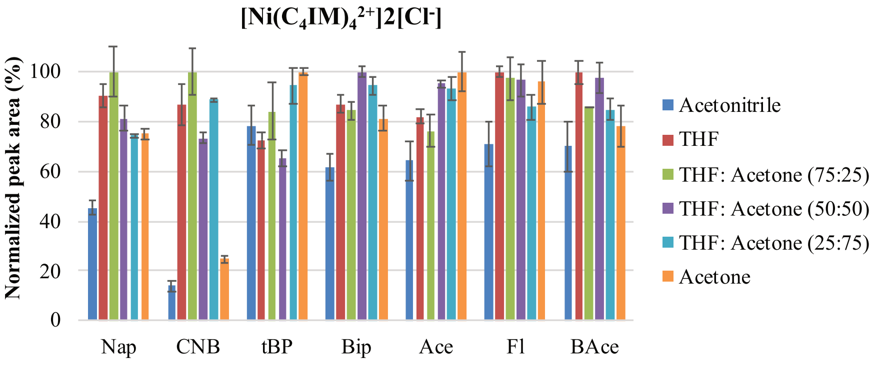

Fig. 3. Effect of dispersive solvent type in the *in situ* SBDLLME method using the $[\mathrm{Ni(C_8IM)_4}^{2+}]2[\mathrm{Cl}^-]$ MIL. *Experimental conditions* (n = 3): 10 mL sample volume, 500 $\mu\mathrm{g\,L^{-1}}$ as spiked level, pH 2, 18% (w/v) NaCl, 20 mg of MIL, 600 μL of acetonitrile, acetone, tetrahydrofuran (THF), or mixtures as dispersive solvent, 1:2 MIL:$[\mathrm{Li}^+][\mathrm{NTf_2}^-]$ molar ratio and stirring (1150 rpm, 5 min).

Table 2
Analytical performance of the developed *in situ* SBDLLME method using different MILs.

Analyte	$[Ni(C_4IM)_4^{2+}]2[Cl^-]$				$[Ni(C_8IM)_4^{2+}]2[Cl^-]$				$[Co(C_8IM)_4^{2+}]2[Cl^-]$			
	Linear range ($\mu g\,L^{-1}$)	LOD[a] ($\mu g\,L^{-1}$)	RSD[b] (%)	RR[c] (%)	Linear range ($\mu g\,L^{-1}$)	LOD[a] ($\mu g\,L^{-1}$)	RSD[b] (%)	RR[c] (%)	Linear range ($\mu g\,L^{-1}$)	LOD[a] ($\mu g\,L^{-1}$)	RSD[b] (%)	RR[c] (%)
Nap	15–1000	4.8	12	96.7	15–1000	4.0	1.8	77.5	15–800	7.0	6.7	78.8
CNB	30–800	11	15	104	50–1000	10	10	88.0	15–800	7.0	5.6	70.0
tBP	45–800	15	7.0	75.2	15–1000	6.4	0.5	96.8	25–800	30	6.9	108
Bip	15–1000	5.6	3.1	109	50–800	3.0	6.8	72.5	15–800	5.9	6.0	80.6
Ace	15–1000	5.0	4.3	102	15–1000	2.0	6.9	90.0	15–800	7.5	3.4	76.3
Fl	15–800	5.6	2.3	107	15–800	3.4	9.4	103	15–800	6.8	5.5	72.1
BAce	15–1000	5.5	4.1	73.7	15–800	5.0	10	81.4	15–800	20	4.4	90.8

[a] Limit of detection, calculated as 3 times the signal-to-noise ratio.
[b] Relative standard deviation (spiked level of 80 $\mu g\,L^{-1}$, n = 3).
[c] Relative recovery (spiked level of 80 $\mu g\,L^{-1}$).

extraction of this group of analytes, likely due to additional hydrophobic interactions between the alkyl chains of the ligands and the analytes. The results proved that the metal center of the MIL also played a role in the extraction of the target analytes. Therefore, the presence of the Ni^{2+} metal center in the MIL cation provided higher calibration slopes, likely because the dispersion of these MILs was more effective due to their lower tendency to stick on the glass surface.

LODs and LOQs were determined as the concentration corresponding to three and ten times the signal-to-noise ratio, respectively, and were experimentally confirmed. Low LODs were achieved in this method, ranging between 4.8 and 15 $\mu g\,L^{-1}$ for the $[Ni(C_4IM)_4^{2+}]2[Cl^-]$ MIL, 2.0–10 $\mu g\,L^{-1}$ for the $[Ni(C_8IM)_4^{2+}]2[Cl^-]$ MIL, and 5.9–30 $\mu g\,L^{-1}$ for the $[Co(C_8IM)_4^{2+}]2[Cl^-]$ MIL (see Table 2).

The reproducibility was estimated as the relative standard deviation (RSD) for a spiked level of 80 $\mu g\,L^{-1}$ (n = 3). The RSD ranged between 2.3% and 10%, 0.5–10%, and 3.4–6.9% for the $[Ni(C_4IM)_4^{2+}]2[Cl^-]$, $[Ni(C_8IM)_4^{2+}]2[Cl^-]$, and $[Co(C_8IM)_4^{2+}]2[Cl^-]$ MILs, respectively.

The RR values, expressed as a percentage, were calculated as the ratio from the predicted concentration obtained using the calibration curves of the entire method (Tables S3, S4 and S5 of the SM) and the spiked concentration. The RR values ranged between 73.7% and 109% for the $[Ni(C_4IM)_4^{2+}]2[Cl^-]$ MIL, 72.5–102% for the $[Ni(C_8IM)_4^{2+}]2[Cl^-]$ MIL, and 70.0–108% for the $[Co(C_8IM)_4^{2+}]2[Cl^-]$ MIL.

The developed method was compared with other reported methods of the literature [4,5,14,15,25,26], as Table S6 of the SM shows. Previously reported DLLME, single drop microextraction (SDME) and SBDLME methods utilized hydrophobic MILs as extraction solvents [4,5,14,25,26]. In comparison, the hydrophobic MILs used in this approach are generated *in situ* during the microextraction procedure, which was shown to improve the extraction efficiency in previous studies [19,27–29]. In these cases, the metathesis reaction maximized the interface between phases and accelerated the mass transfer of analytes into the extraction solvent. In addition, the proposed method provides enormous advantages for its combination with HS-GC-MS. Thus, previous generations of MILs generally generate higher MIL background in the GC-MS due to decomposition of the MIL anion during the HS sampling step [15]. For comparison purposes, Fig. S10 of the SM shows a comparison of the background provided by the previous generations of MILs used in SBDLLME and the $[Ni(C_8IM)_4^{2+}]2[NTf_2^-]$ MIL used in this application. As an additional advantage, the *in situ* SBDLLME method can be easily automated [30].

3.4. Analysis of real samples

The method was applied for the analysis of water samples, including tap and mineral water. No analytes were detected in the samples using any of the studied MILs. For that reason, spiked samples were analyzed to examine any matrix effects that these samples exert in the determination of the analytes. Table 3 shows the obtained results regarding the reproducibility and the RR using a spiked level of 80 $\mu g\,L^{-1}$ (n = 3). RSD values lower than 16% were obtained for both tap and mineral water. Furthermore, acceptable RR values were obtained for the majority of the analytes, except for tBP in tap water using the $[Ni(C_4IM)_4^{2+}]2[Cl^-]$ MIL; CNB in tap water and mineral water and tBP in mineral water using the $[Ni(C_8IM)_4^{2+}]2[Cl^-]$ MIL; and tBP and Ace in tap water employing the $[Co(C_8IM)_4^{2+}]2[Cl^-]$ MIL. In these cases, the matrix effect was significant, indicating that matrix matched calibration or standard addition is required for quantification of analytes.

4. Conclusions

A new generation of MILs containing paramagnetic cations able to

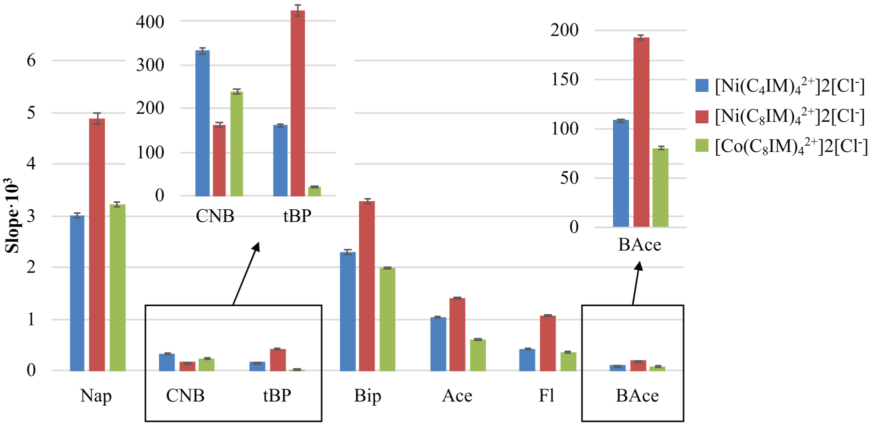

Fig. 4. Calibration slopes obtained during the validation of the entire *in situ* SBDLLME-HS-GC-MS method using different MILs.

Table 3
Analysis of real samples using the *in situ* SBDLLME method with different MILs.

Analyte	$[Ni(C_4IM)_4^{2+}]\,2\,[Cl^-]$				$[Ni(C_8IM)_4^{2+}]\,2\,[Cl^-]$				$[Co(C_8IM)_4^{2+}]\,2\,[Cl^-]$			
	Tap water		Mineral water		Tap water		Mineral water		Tap water		Mineral water	
	RSD[a] (%)	RR[b] (%)	RSD[a] (%)	RR[b] (%)	RSD[a] (%)	RR[b] (%)	RSD[a] (%)	RR[b] (%)	RSD[a] (%)	RR[b] (%)	RSD[a] (%)	RR[b] (%)
Nap	8.5	95.7	13	88.8	3.4	98.0	7.5	83.8	2.2	93.0	2.1	96.5
CNB	9.2	104	4.0	115	10	52.0[c]	12	59.6[c]	9.6	95.1	7.8	100
tBP	16	7.87[c]	17	86.9	12	75.0	14	56.3[c]	7.8	43.3[c]	7.7	102
Bip	4.0	112	2.2	101	5.4	88.6	6.3	112	10	91.7	7.4	94.6
Ace	10	75.8	3.8	100	13	94.2	13	96.2	4.2	44.2[c]	4.0	106
Fl	3.4	106	1.8	91.9	3.3	101	7.6	118	6.5	90.4	5.0	89.9
BAce	1.1	92.2	6.9	110	8.0	96.7	9.4	94.9	14	96.2	16	103

*Spiked level of 80 $\mu g\,L^{-1}$, n = 3.
[a] Relative standard deviation.
[b] Relative recovery.
[c] Matrix effect was significant for the specific analyte and MIL.

perform *in situ* metathesis reaction during the microextraction procedure was developed. The MILs selected in this study were specifically designed to contain different metal centers (Ni^{2+} or Co^{2+}) and N-alkylimidazole ligands (C_4IM or C_8IM), and were successfully applied for *in situ* SBDLLME in combination with HS-GC-MS.

The thermal stability of the $[NTf_2^-]$-based MILs was studied by HS-GC-MS, with the $[Ni(C_8IM)_4^{2+}]2[NTf_2^-]$ MIL being the most thermally stable compound. The obtained results indicated that the coordination between Ni^{2+} and the nitrogen atoms of the N-alkylimidazole ligands is stronger than the corresponding Co^{2+}–N coordination, but also revealed that long alkyl chains substituents in the ligand can increase the thermal stability of the MILs.

Optimization studies of the *in situ* SBDLLME method revealed that the extraction behavior of the MILs containing N-octylimidazole was similar, indicating that the type of ligand in the MIL structure plays an important role in the optimum extraction conditions required for the method.

The *in situ* SBDLLME method was successfully validated for each of the studied MILs, with LODs lower than 15, 10, and 30 $\mu g\,L^{-1}$ for the $[Ni(C_4IM)_4^{2+}]2[Cl^-]$, $[Ni(C_8IM)_4^{2+}]2[Cl^-]$, and $[Co(C_8IM)_4^{2+}]2[Cl^-]$ MILs, respectively, and RSD lower than 10% obtained in all cases. The best extraction performance was achieved using the $[Ni(C_8IM)_4^{2+}]2[Cl^-]$ MIL, likely due to its capability in promoting additional hydrophobic interactions with analytes, and also due to the nature of the Ni^{2+} metal center.

The method was successfully applied for the analysis of water samples including both tap and mineral water, with RSD values lower than 17% obtained in all cases, and acceptable RR values for the majority of the analytes. Ongoing work is focused on automating the microextraction procedure as well as the analysis of different types of samples.

Acknowledgements

JLA acknowledges funding from Chemical Measurement and Imaging Program at the National Science Foundation (Grant number CHE-1709372)

Appendix A. Supporting information

Supplementary data associated with this article can be found in the online version at doi:10.1016/j.talanta.2018.12.071.

References

[1] J. He, M. Huang, D. Wang, Z. Zhang, G. Li, Magnetic separation techniques in sample preparation for biological analysis: a review, J. Pharm. Biomed. Anal. 101 (2014) 84–101, https://doi.org/10.1016/j.jpba.2014.04.017.

[2] J.L. Benedé, A. Chisvert, D.L. Giokas, A. Salvador, Development of stir bar sorptive-dispersive microextraction mediated by magnetic nanoparticles and its analytical application to the determination of hydrophobic organic compounds in aqueous media, J. Chromatogr. A 1362 (2014) 25–33, https://doi.org/10.1016/j.chroma.2014.08.024.

[3] J.L. Benedé, A. Chisvert, D.L. Giokas, A. Salvador, Determination of ultraviolet filters in bathing waters by stir bar sorptive–dispersive microextraction coupled to thermal desorption– gas chromatography–mass spectrometry, Talanta 147 (2016) 246–252, https://doi.org/10.1016/j.talanta.2015.09.054.

[4] A. Chisvert, J.L. Benedé, J.L. Anderson, S.A. Pierson, A. Salvador, Introducing a new and rapid microextraction approach based on magnetic ionic liquids: stir bar dispersive liquid microextraction, Anal. Chim. Acta 983 (2017) 130–140, https://doi.org/10.1016/j.aca.2017.06.024.

[5] J.L. Benedé, A. Chisvert, J.L. Anderson, Trace determination of volatile polycyclic aromatic hydrocarbons in natural waters by magnetic ionic liquid-based stir bar dispersive liquid microextraction, Talanta 176 (2018) 253–261, https://doi.org/10.1016/j.talanta.2017.07.091.

[6] J.M.F. Nogueira, Stir-bar sorptive extraction: 15 years making sample preparation more environment-friendly, Trends Anal. Chem. 71 (2015) 214–223, https://doi.org/10.1016/j.trac.2015.05.002.

[7] N. Reyes-Garces, E. Gionfriddo, G.A. Goḿez-Ríos, M.N. Alam, E. Boyacı, B. Bojko, V. Singh, J. Grandy, J. Pawliszyn, Advances in solid phase microextraction and perspective on future directions, Anal. Chem. (2018) 302–360, https://doi.org/10.1021/acs.analchem.7b04502.

[8] M. Leong, M. Fuh, S. Huang, Beyond dispersive liquid – liquid microextraction, J. Chromatogr. A 1335 (2014) 2–14, https://doi.org/10.1016/j.chroma.2014.02.021.

[9] L. Mousavi, Z. Tamiji, M.R. Khoshayand, Applications and opportunities of experimental design for the dispersive liquid–liquid microextraction method – a review, Talanta 190 (2018) 335–356, https://doi.org/10.1016/j.talanta.2018.08.002.

[10] K.D. Clark, O. Nacham, J.A. Purslow, S.A. Pierson, J.L. Anderson, Magnetic ionic liquids in analytical chemistry: a review, Anal. Chim. Acta 934 (2016) 9–21.

[11] E. Santos, J. Albo, A. Irabien, Magnetic ionic liquids: synthesis, properties and applications, RSC Adv. 4 (2014) 40008–40010, https://doi.org/10.1016/j.aca.2016.06.011.

[12] M.J. Trujillo-Rodríguez, H. Nan, M. Varona, M.N. Emaus, I.D. Souza, J.L. Anderson, Advances of ionic liquids in analytical chemistry, Anal. Chem. (2019), https://doi.org/10.1021/acs.analchem.8b04710 (In press).

[13] S.A. Pierson, O. Nacham, K.D. Clark, H. Nan, Y. Mudryk, J.L. Anderson, Synthesis and characterization of low viscosity hexafluoroacetylacetonate-based hydrophobic magnetic ionic liquids, New J. Chem. 41 (2017) 5498–5505, https://doi.org/10.1039/C7NJ00206H.

[14] T. Chatzimitakos, S.A. Pierson, J.L. Anderson, C. Stalikas, Enhanced magnetic ionic liquid-based dispersive liquid-liquid microextraction of triazines and sulfonamides through a one-pot, pH-modulated approach, J. Chromatogr. A 1571 (2018) 47–54, https://doi.org/10.1016/j.chroma.2018.08.013.

[15] M.J. Trujillo-Rodríguez, V. Pino, J.L. Anderson, Magnetic ionic liquids as extraction solvents in vacuum headspace single-drop microextraction, Talanta 172 (2017) 86–94, https://doi.org/10.1016/j.talanta.2017.05.021.

[16] M.N. Emaus, K.D. Clark, P. Hinners, J.L. Anderson, Preconcentration of DNA using magnetic ionic liquids that are compatible with real-time PCR for rapid nucleic acid quantification, Anal. Bioanal. Chem. 410 (2018) 4135–4144, https://doi.org/10.1007/s00216-018-1092-9.

[17] X. Peng, K.D. Clark, X. Ding, C. Zhu, M. Varona, M.N. Emaus, J. An, J.L. Anderson, Coupling oligonucleotides possessing a poly-cytosine tag with magnetic ionic liquids for sequence-specific DNA analysis, Chem. Commun. 54 (2018) 10284–10287, https://doi.org/10.1039/C8CC05954C.

[18] D. Chand, M.Q. Farooq, A.K. Pathak, J. Li, E.A. Smith, J.L. Anderson, Magnetic ionic liquids based on transition-metal complexes with N-alkylimidazole ligands, New J. Chem. 43 (2019) 20–23, https://doi.org/10.1039/C8NJ05176C.

[19] M.J. Trujillo-Rodríguez, J.L. Anderson, *In situ* formation of hydrophobic magnetic ionic liquids for dispersive liquid-liquid microextraction, in press, J. Chromatogr. A

(2019), https://doi.org/10.1016/j.chroma.2018.12.032.

[20] C. Zhang, C. Cagliero, S.A. Pierson, J.L. Anderson, Rapid and sensitive analysis of polychlorinated biphenyls and acrylamide in food samples using ionic liquid-based in situ dispersive liquid-liquid microextraction coupled to headspace gas chromatography, J. Chromatogr. A 1481 (2017) 1–11, https://doi.org/10.1016/j.chroma.2016.12.013.

[21] T.D. Ho, P.M. Yehl, N.P. Chetwyn, J. Wang, J.L. Anderson, Q. Zhong, Determination of trace level genotoxic impurities in small molecule drug substances using conventional headspace gas chromatography with contemporary ionic liquid diluents and electron capture detection, J. Chromatogr. A 1361 (2014) 217–228, https://doi.org/10.1016/j.chroma.2014.07.099.

[22] S.A. Pierson, M.J. Trujillo-Rodríguez, J.L. Anderson, Rapid analysis of ultraviolet filters using dispersive liquid – liquid microextraction coupled to headspace gas chromatography and mass spectrometry, J. Sep. Sci. 41 (2018) 3081–3088, https://doi.org/10.1002/jssc.201800415.

[23] B. Lenarcik, T. Rauckyte, The influence of alkyl chain length on extraction equilibria of Ni(II) complexes with 1-alkylimidazoles in aqueous solution/organic solvent systems, Sep. Sci. Technol. 39 (2004) 3353–3372, https://doi.org/10.1081/SS-200028915.

[24] B. Lenarcik, P. Ojczenasz, Investigation of the stability of Co(II) complexes with a homologous series of 1-alkylimidazoles in aqueous solution by using a partition method with several solvents, Sep. Sci. Technol. 39 (2004) 199–226, https://doi.org/10.1081/SS-120027409.

[25] M.J. Trujillo-Rodríguez, O. Nacham, K.D. Clark, J.L. Anderson, J.H. Ayala, A.M. Afonso, Magnetic ionic liquids as non-conventional extraction solvents for the determination of polycyclic aromatic hydrocarbons, Anal. Chim. Acta 934 (2016) 106–113, https://doi.org/10.1016/j.aca.2016.06.014.

[26] J. An, K.L. Rahn, J.L. Anderson, Headspace single drop microextraction versus dispersive liquid-liquid microextraction using magnetic ionic liquid extraction solvents, Talanta 167 (2017) 268–278, https://doi.org/10.1016/j.talanta.2017.01.079.

[27] M. Baghdadi, F. Shemirani, *In situ* solvent formation microextraction based on ionic liquids: a novel sample preparation technique for determination of inorganic species in saline solutions, Anal. Chim. Acta 634 (2009) 186–191, https://doi.org/10.1016/j.aca.2008.12.017.

[28] C. Yao, J.L. Anderson, Dispersive liquid – liquid microextraction using an *in situ* metathesis reaction to form an ionic liquid extraction phase for the preconcentration of aromatic compounds from water, Anal. Bioanal. Chem. 395 (2009) 1491–1502, https://doi.org/10.1007/s00216-009-3078-0.

[29] T. Li, M.D. Joshi, D.R. Ronning, J.L. Anderson, Ionic liquids as solvents for in situ dispersive liquid-liquid microextraction of DNA, J. Chromatogr. A 1272 (2013) 8–14, https://doi.org/10.1016/j.chroma.2012.11.055.

[30] M. Sajid, J. Płotka-Wasylka, Combined extraction and microextraction techniques: recent trends and future perspectives, Trac – Trends Anal. Chem. 103 (2018) 74–86, https://doi.org/10.1016/j.trac.2018.03.013.